Convection-enhanced delivery of nanoliposomal CPT-11 (irinotecan) and PEGylated liposomal doxorubicin (Doxil) in rodent intracranial brain tumor xenografts

Michal T. Krauze, Charles O. Noble, Tomohiro Kawaguchi, Daryl Drummond, Dmitri B. Kirpotin, Yoji Yamashita, Erika Kullberg, John Forsayeth, John W. Park, and Krystof S. Bankiewicz

Department of Neurological Surgery, Brain Tumor Research Center (M.T.K., T.K., Y.Y., J.F., K.S.B.), and Division of Hematology-Oncology (C.O.N., E.K., J.W.P.), University of California, San Francisco, San Francisco, CA; Hermes Biosciences, Inc., South San Francisco, CA (C.O.N., D.D., D.B.K.); USA

We have previously shown that convection-enhanced delivery (CED) of highly stable nanoparticle/liposome agents encapsulating chemotherapeutic drugs is effective against intracranial rodent brain tumor xenografts. In this study, we have evaluated the combination of a newly developed nanoparticle/liposome containing the topoisomerase I inhibitor CPT-11 (nanoliposomal CPT-11 [nLs-CPT-11]), and PEGylated liposomal doxorubicin (Doxil) containing the topoisomerase II inhibitor doxorubicin. Both drugs were detectable in the CNS for more than 36 days after a single CED application. Tissue half-life was 16.7 days for nLs-CPT-11 and 10.9 days for Doxil. The combination of the two agents produced synergistic cytotoxicity in vitro. In vivo in U251MG and U87MG intracranial rodent xenograft models, CED of the combination was also more efficacious than either agent used singly. Analysis of the parameters involved in this approach indicated that tissue pharmacokinetics, tumor microanatomy, and biochemical interactions of the drugs all contributed to the therapeutic efficacy observed. These findings have implications for further clinical applications of CED-based treatment of brain tumors. *Neuro-Oncology 9, 393–403, 2007 (Posted to Neuro-Oncology [serial online], Doc. D06-00150, July 24, 2007. URL http://neuro-oncology.dukejournals.org; DOI: 10.1215/15228517-2007-019)*

Keywords: brain tumor, CED, CPT-11, Doxil, irinotecan, liposome, xenograft

Despite intensive multimodal treatment such as surgical resection, radiation therapy, and systemic chemotherapy, malignant brain tumors (e.g., glioblastoma multiforme) remain the most difficult neoplasms to treat. Poor penetration of the blood–brain barrier (BBB) by many anticancer drugs results in the need for high doses of systemic chemotherapeutics.[1,2] Systemic side effects are therefore the limiting factor in chemotherapeutic protocols for brain tumor patients. Intratumoral chemotherapy has been proposed in order to overcome these difficulties and in recognition of clinical observations that 90% of malignant gliomas recur within 2 cm of an original resection site.[3] However, many local drug delivery techniques face the persistent problem of poor distribution of infused drugs.[4] Convection-enhanced delivery (CED) was introduced by Bobo et al.[5] to overcome this difficulty. CED is a direct infusion technique that utilizes bulk flow to deliver molecules to a

Received August 31, 2006; accepted December 18, 2006.

Address correspondence to Krystof S. Bankiewicz, Department of Neurological Surgery, MCB226, University of California, San Francisco, 1855 Folsom St., Mission Center Building, San Francisco, CA 94103-0555, USA (krystof.bankiewicz@ucsf.edu).

targeted site, offering an improved volume of distribution over that of simple diffusion. CED of therapeutic agents bypasses the BBB, delivers a high concentration of therapeutic agents to the infusion site, provides a wider distribution of therapeutic agents within the target site, and minimizes systemic exposure, resulting in fewer systemic toxicities.[6–9] Promising results have been reported from clinical trials with CED of several therapeutic agents in malignant brain tumors.[10–13] A major disadvantage of all these clinical trials is that delivery to the CNS cannot be monitored in real time. Therefore, side effects (e.g., chemical meningitis) can be explained only empirically.

In order to further improve the clinical prospects for CED-based therapy, we have introduced a number of innovations to CED for both current and future clinical applications. We have defined four steps essential for more efficient brain tumor therapies in the future: (1) visualized controlled local delivery of therapeutic agents to the CNS, (2) highly active therapeutic combinations that display relatively low toxicity in healthy brain, (3) optimized pharmacokinetic profile of the therapeutic agent that allows for a long half-life of the active agent in the brain in order to alleviate the need for frequent dosing and to introduce metronomic chemotherapy that targets dormant cancer cells as well as the supporting angiogenic blood vessels, and (4) establishment of therapeutic delivery parameters flexible enough to accommodate multiple tumor types.

Liposomes provide stable encapsulation for various anticancer drugs and have a number of advantages over the corresponding free drugs for the systemic treatment of cancer.[14,15] Liposomal drugs are promising candidates for local delivery within the CNS, because they are inert until the drug is made bioavailable via release from the carrier. Liposomes now also play an important role in neuro-oncology not only because of their pharmacokinetic profile but also because their distribution in the CNS can be visualized by MRI.[16,17] The introduction of a novel step-design delivery catheter in our CED studies provided for distribution of the therapeutic agent, free of detectable reflux at any infusion rate examined thus far, up to 50 μl/min.[18] We have previously shown excellent distribution of liposomes throughout the primate brain with this catheter.[17] Considerable progress has been reported in developing real-time imaging strategies with liposomal MRI contrast agents in primate CNS.[16,17,19]

Drug delivery kinetics to the brain have been optimized by encapsulation of small-molecule drugs in liposomes, thereby markedly improving the pharmacokinetic profile of these drugs in the CNS.[8] A unique intraliposomal stabilization technology has resulted in stable controlled-release formulations for a variety of difficult-to-encapsulate drugs, for example, irinotecan.[20,21] We have previously evaluated in separate studies liposomes containing either the topoisomerase I (Topo I) inhibitor doxorubicin[9] or the topoisomerase II (Topo II) inhibitors CPT-11 and topotecan, against human brain tumor xenografts.[8,22] Results from these studies have been encouraging, in part because Topo I and Topo II inhibitors exert their principal effects on the two major classes of enzymes involved in regulating DNA topology. This functional overlap suggested that a combination of both drugs could act synergistically against orthotopic brain tumor xenografts. Administration of a combination of nonliposomal Topo I and Topo II inhibitors to patients with advanced solid malignancies has been evaluated in numerous clinical studies.[23–25]

In this study, we evaluated PEGylated liposomal doxorubicin (Doxil) and nanoliposomal CPT-11 (nLs-CPT-11) in vitro and in vivo with respect to toxicity, tissue half-life, and efficacy in U87MG and U251MG xenografts. We demonstrated that only distribution within the entire tumor is able to prolong animal survival in the rodent brain tumor xenograft model.

Materials and Methods

Liposomal Therapeutics

Control "empty" liposomes, not loaded with drug, were composed of L-α-distearoylphosphatidylcholine (DSPC), choline (Chol), 1,1'-dioctadecyl-2,3,3',3'-tetramethylindocarbocyanine perchlorate [$DiIC_{18}(3)$], and polyethylene glycol–coupled 1,2-distearoyl-sn-glycero-3-phosphatidylethanolamine (PEG-DSPE) in the molar ratio of 3:2:0.03:0.015. nLs-CPT-11 was composed of DSPC, Chol, and PEG-DSPE at a molar ratio of 3:2:0.015. Liposomes were prepared by dissolution of all lipids in chloroform/methanol (9:1, vol/vol) and subsequent removal of the solvent by rotary evaporation to form a dried lipid foam. The dried lipids were hydrated in 81 mM aqueous triethylammonium sucrose octasulfate solution (0.65 M triethylamine, pH 5.2) at 60°C, and the hydrated lipid suspension was subjected to eight cycles of freezing (–80°C) and thawing (60°C). After hydration, trace organic solvent was removed from the lipid suspension on a rotary evaporator. Unilamellar liposomes were formed by extrusion at 60°C in a pressurized, thermostat-controlled barrel extruder (Lipex Biomembranes, Vancouver, Canada) through double-stacked polycarbonate membranes (Whatman Nucleopore, Clifton, NJ, USA) of pore size 200 nm (6 times) and 100 nm (12 times), yielding a final liposomal diameter of 95–110 nm as determined by dynamic light scattering (N4Plus particle size analyzer; Beckman Coulter, Fullerton, LA, USA). Extraliposomal triethylammonium sucrose octasulfate was removed by size-exclusion chromatography on a Sepharose CL-4B column eluted with HEPES-buffered dextrose (5 mM HEPES, 5% dextrose, pH 6.5).

CPT-11 was loaded into the liposomes by addition of a 15 mg/ml solution of CPT-11·HCl to a final drug-to-lipid ratio of 750 g CPT-11·HCl per mole of phospholipid, and incubation of the drug/liposome mixture at 60°C for 45 min, followed by quenching on ice for 15 min. Unencapsulated CPT-11 was removed by chromatography on a Sephadex G-75 size-exclusion column that was eluted with HEPES-buffered saline (5 mM HEPES, 145 mM NaCl, pH 6.5). Drug-loaded liposomes were stored at 4°C until use. Drug-loading efficiencies of >95% were typically observed. Nanoliposomal CPT-11 (nLs-CPT-11)

was concentrated on a stirred cell concentrator (Millipore Corp., Billerica, MA, USA) containing a regenerated cellulose 1×10^5 nominal molecular-weight-limit membrane (Millipore) and sterilized by passage through a 0.2-μm polyethersulfone syringe filter. The concentration of CPT-11 was determined by measuring the absorbance at 375 nm of a solubilized liposome sample. Briefly, 0.1 ml of an aqueous portion of the sample containing nLs-CPT-11 or standards was added to 0.9 ml of a solution containing 72 vol% methanol, 18 vol% 0.1 M phosphoric acid, and 10 vol% chloroform. Phospholipid was measured by a spectrophotometric assay.[26] All drug values for nLs-CPT-11 in this manuscript refer to equivalents of CPT-11·HCl.[8]

PEGylated liposomal doxorubicin was obtained as Doxil (Alza Pharmaceuticals, Mountain View, CA, USA). All drug values for Doxil refer to equivalents of doxorubicin·HCl.[9]

Tumor Cell Lines

Human glioblastoma multiforme cell lines U87MG and U251MG were obtained from the Brain Tumor Research Center Tissue Bank at the University of California, San Francisco (UCSF). Cells were maintained as monolayers in Eagle's minimal essential medium supplemented with 10% fetal calf serum, antibiotics, and nonessential amino acids. Cells were cultured at 37°C in a humidified atmosphere of 95% air and 5% CO_2.

Cell Cycle Analysis

One day prior to treatment, 2×10^5 cells were seeded into each well of a six-well plate (Corning Inc., Corning, NY, USA). Cells were exposed to drug-free $DiIC_{18}(3)$-DS liposomes (control liposomes), Doxil (0.2 μg doxorubicin/ml), nLs-CPT-11 (1 μg CPT-11/ml), or both, in complete medium. After 24 h, cells were fixed in 70% ethanol, washed, digested with RNase A (Sigma, St. Louis, MO, USA), stained with propidium iodide (Sigma), and subjected to flow cytometry in a FACScan (Becton-Dickinson, San Jose, CA, USA) with 10,000 events/determination. ModFit LT software (Verity Software House, Inc., Topsham, ME, USA) analyzed cell cycle distribution.

Cell Viability Assay

Cells were seeded at 1,000 cells/well in 96-well plates (Corning Inc.), allowed to attach for 24 h, and then exposed to drug-free $DiIC_{18}(3)$-DS liposomes (control liposomes), Doxil, nLs-CPT-11, or both, in complete medium. For combination studies, the ratio of Doxil to nLs-CPT-11 was kept constant at 1:5 (wt/wt of doxorubicin to CPT-11). MTT [3-(4, 5-dimethylthiazol-2-yl)-5-(3-carboxymethoxyphenyl)-2-(4-sulfophenyl)-2H-tetrazolium] reagent was added 48 h after initiation of treatment, and plates were read at an absorbance of 490 nm 3 h later with a SpectraMax microplate reader (Molecular Devices Corporation, Sunnyvale, CA, USA). All treatments were performed in triplicate. The background absorbance was determined by incubating media with substrate alone and subtracting the values from wells containing cells only.

Animals and Intracranial Xenograft Technique

Male Sprague-Dawley rats (250 g) were obtained from Charles River Laboratories (Wilmington, MA, USA). Congenitally athymic, male, homozygotic, nude rats (*rnu/rnu*; 150–200 g) were purchased from the National Cancer Institute Animal Production Program (Frederick, MD, USA) and were housed under aseptic conditions. All protocols were approved by the Institutional Animal Care and Use Committee at UCSF. For the intracranial xenograft tumor model, U87MG and U251MG cells were harvested by trypsinization, washed once with Hank's balanced salt solution without Ca^{2+} and Mg^{2+} (HBSS), and resuspended in HBSS for implantation. A cell suspension of 5×10^5 cells/10 μl HBSS was implanted into the striatal region of the athymic rat brains. Under isoflurane anesthesia, rats were placed in a small-animal stereotactic frame (David Kopf Instruments, Tujunga, CA, USA). A sagittal incision was made to expose the cranium, and a burr-hole was made in the skull 0.5 mm anterior and 3 mm lateral from the bregma. At a depth of 4.5 mm below the brain surface, 5 μl of cell suspension was injected. Two minutes later, the needle tip was elevated 0.5 mm, and another 5 μl was injected at a depth of 4 mm. After a further 2 min, the needle was removed and the wound sutured.

Convection-Enhanced Delivery

Throughout this study, drugs were delivered in a volume of 20 μl by CED as described previously.[6,27] Briefly, a fused-silica cannula was connected to a loading line (containing liposomes) and an oil-infusion line. A 1-ml syringe (filled with oil) was mounted onto a microinfusion pump (BeeHive; Bioanalytical Systems, West Lafayette, IN, USA) that regulated the flow of fluid through the system. Based on tumor injection site coordinates, a reflux-free and backflow-free step-design cannula[18] was mounted onto stereotactic holders and guided to the targeted region (4.5 mm depth) of the brain through burr holes made in the skull as described above. An infusion rate of 0.5 μl/min over 40 min was applied to achieve a final infusion volume of 20 μl.

Tissue Pharmacokinetics

Rats were given a single 20-μl infusion by CED of Doxil (2 mg, 0.1 mg/ml) together with nLs-CPT-11 (0.8 mg, 40 mg/ml), and the animals were sacrificed at prescribed times. The brain hemisphere was perfused with phosphate-buffered saline, surgically removed, and frozen. Water was added to the tissue at a 50% wt/wt ratio, and the tissue was homogenized mechanically in an ice bath. The homogenates (0.1 ml) were extracted with 0.9 ml of chloroform/methanol (4:1) by vortexing for 15 s, and the organic phase was collected. This process was repeated, and the combined organic extracts were evaporated to dryness with a centrifugal concentrator. The residue was

dissolved in 0.5 ml methanol, and centrifuged at 10,000 rpm for 10 min. The supernatant solution was analyzed by high-performance liquid chromatography (HPLC). Standards were prepared by extraction of spiked blank tumor tissue. Analysis was conducted on a Dionex HPLC system with a C_{18} reverse-phase silica column (Supelco C-18 column, 250 mm × 4 mm inner diameter, 5 mm particle size), preceded by a Supelco C_{18} guard column. A sample injection volume of 50 μl was used, and the column was eluted at a flow rate of 1.0 ml/min with a mobile phase consisting of 0.21 M aqueous triethylammonium acetate (pH 5.5) and acetonitrile. A linear gradient elution was used with the acetonitrile content increasing from 27% to 45% over 10 min. Each drug was detected by a fluorescence detector (excitation, 485 nm; emission, 590 nm). Typical retention times for CPT-11 and doxorubicin were 5.4 min and 7.1 min, respectively.

Pharmacokinetic parameters that included the tissue half-lives of the drug ($t_{1/2}$), clearance, the mean residence time in the brain or brain/tumor, and the area under the concentration versus time curve were all determined by noncompartmental pharmacokinetic data analysis with PK Solutions 2.0 software (Summit Research Services, Montrose, CO, USA).

Evaluation of Toxicity

Three normal Sprague-Dawley rats were evaluated for potential local toxicity after CED-mediated co-infusion of Doxil and nLs-CPT-11. Rats were monitored daily for general health (alertness, grooming, feeding, excreta, skin, fur, mucous membranes, ambulation, breathing, and posture). Animal weights were reported weekly. Doxil was used at 50% of the maximum tolerated dose (MTD), determined previously.[9] Little nLs-CPT-11 toxicity has been observed in previous studies, and the drug was used at a safe dose determined previously.[8] Sixty days after CED of a 20-μl solution containing Doxil (2 mg, 0.1 mg/ml) and nLs-CPT-11 (0.8 mg, 40 mg/ml) into the striatum, rats were euthanized and their brains fixed in 4% formaldehyde. Fixed brain tissue was subjected to paraffin sectioning (5 μm), and sections were stained with hematoxylin and eosin (H&E).

Combination Therapy in the U87MG and U251MG Intracranial Xenograft Models

Forty-two rats were implanted with U251MG tumor cells as described above. Animals treated on day 7 after tumor implantation were randomly divided into four groups: (1) a control consisting of CED of $DiIC_{18}(3)$-DS fluorescent liposomes (n = 6), (2) CED of Doxil (n = 6), (3) CED of nLs-CPT-11 (n = 6), and (4) a combination treatment of Doxil together with nLs-CPT-11 (n = 6). In a second study, animals were randomly divided into two groups on day 14 after tumor implantation: a control consisting of CED of drug-free liposomes (n = 9) and a combination treatment of Doxil and nLs-CPT-11 (n = 9).

In a third study, 24 rats implanted with U87MG tumor cells were randomly divided into four groups on day 10 after tumor implantation: (1) a control group consisting of drug-free liposomes (n = 6), (2) CED of Doxil (n = 6), (3) CED of nLs-CPT-11, and (4) a combination treatment of Doxil and nLs-CPT-11 (n = 6). CED of 20 μl of the specified drug was performed for each group in all survival studies. Rats were monitored daily for survival and general health (alertness, grooming, feeding, excreta, skin, fur, mucous membrane conditions, ambulation, breathing, and posture). Animal weights were reported weekly. The studies in U251MG were terminated 100 days after tumor implantation, and the U87MG survival study was terminated 70 days after tumor implantation. Surviving animals were euthanized, and their brains were sectioned and stained with H&E.

Distribution of Liposomes in U87MG and U251MG Brain Tumor Xenografts

Animals were implanted with U87MG (n = 3) and U251MG (n = 3) tumor cells. CED with 20 μl of $DiIC_{18}(3)$-DS fluorescent liposomes was performed on day 10 after implantation of U87MG and on day 30 after tumor implantation of U251MG. Animals were euthanized immediately after the infusion procedure. Brains were frozen and cut into 25-μm sections on a cryostat. Fluorescent images of liposome distribution were taken of each brain from rostral to caudal in 100-μm intervals. The fluorescent signal generated by $DiIC_{18}(3)$ was visualized with a fluorescence microscope equipped with a 540/25 nm band-pass filter for excitation, together with a long-pass filter at 565 nm for emission. A charge-coupled device camera with a fixed aperture was used to capture the image.

Statistical Analysis

Results for the survival studies are expressed as a Kaplan-Meier curve. Survival between the treatment groups was compared with an unpaired Student's t-test and expressed as median survival (MS).

Results

Tissue Pharmacokinetics of Doxil and nLs-CPT-11 Coadministered by CED in Rat Brain

A mixture of liposomes containing 2 mg Doxil and 0.8 mg nLs-CPT-11 was infused by a single CED treatment into the brains of adult rats, and tissue levels were determined by HPLC at various times after infusion (Fig. 1). Both drugs were detectable for more than one month after a single CED treatment. The decline in the tissue concentration of nLs-CPT-11 was exponential (R^2 = 0.9821) with a half-life of 16.7 days (Table 1). Doxil, at a 400-fold lower dose, decreased linearly (R^2 = 0.9975) with a half-life of 10.9 days. The small differences may reflect differences in drug release from the carrier, or differences in clearance of highly PEGylated (Doxil) versus mildly PEGylated liposomes (nLs-CPT-11).

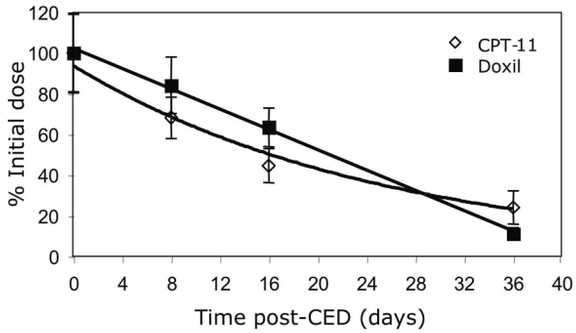

Fig. 1. Tissue pharmacokinetics of nanoliposomal CPT-11 and Doxil in the normal adult rat brain after single convection-enhanced delivery (CED) infusion. All values are percent injected dose versus time after CED of 20 μl infusate. Drug concentrations were determined by high-performance liquid chromatography assay for CPT-11·HCl and doxorubicin·HCl. Values are means ± SD of four animals per time point.

Cell Cycle Distributions In Vitro

Twenty-four hours after treatment of U87MG and U251MG cells with drug-free liposomes (control), Doxil, nLs-CPT-11, or a mixture of the two therapeutic liposomes, changes in cell cycle were recorded (Figs. 2 and 3). U87MG cells exposed to Doxil, a G2/M-active antineoplastic drug, underwent G2 arrest, with the percentage of cells in G2/M increasing from 12% (control) to 46% (Doxil; Fig. 2). U87MG cells exposed to nLs-CPT-11 entered both S-phase, to a marked extent (19% with control liposomes vs. 39% with nLs-CPT-11), and also significant G2 arrest (from 12% with control liposomes to 55% with nLs-CPT-11). After treatment with the combination of Doxil and nLs-CPT-11, both S-phase accumulation and G2 arrest were observed in U87MG cells.

When the same drug concentrations used with U87MG cells were applied to U251MG cells, complete cell cycle arrest was observed (Fig. 3). Doxil, nLs-CPT-11, and the combination of both each caused a complete elimination of cells in S-phase, with virtually all cells in G2 arrest. This difference in tumor cell sensitivity to chemotherapeutics later translated to effects on animal survival (Fig. 4).

Table 1. Tissue pharmacokinetics of nLs-CPT-11 (0.8 mg) and Doxil (2 μg)

	$t_{1/2}$ (d)	AUC (μg·d/g)	CL (g/d)	MRT (d)
nLs-CPT-11	16.7	11,600	0.069	24.1
Doxil	10.9	47.2	0.042	15.8

Pharmacokinetic data from Fig. 1 were analyzed with respect to tissue half-life ($t_{1/2}$), area under the curve (AUC), rate of clearance of either drug from brain tissue (CL), and mean residence time (MRT).

Synergistic Cytotoxic Effects of Doxil and nLs-CPT-11 Liposomes In Vitro (U87MG and U251MG)

Synergy, determined by isobologram analysis,[28] was not observed between the two agents in U87MG cells (Fig. 5). EC_{50} values (median effect doses) calculated from this experiment were 1.18 μg/ml for Doxil and 0.75 μg/ml for nLs-CPT-11. In contrast, synergy was observed between the two agents in U251MG cells (Fig. 5B). EC_{50} values from this experiment were 1.29 μg/ml for Doxil and 0.56 μg/ml for nLs-CPT-11.

Combined Effect of Doxil and nLs-CPT-11 in U251MG and U87MG Brain Tumor Xenografts

First, we studied survival in rodents with intracranial U251MG brain tumor xenografts seven days after tumor cell implantation. Rats that received the control liposomes were all euthanized 36–44 days after tumor cell implantation due to neurological symptoms indicative of tumor progression (Fig. 4). MS for this group was 38.5 days. Three of six rats that received 2 mg Doxil survived until termination of the study. However, neurological symptoms due to large tumor formations were observed in the three remaining rats, which required euthanasia 52–71 days after tumor cell implantation. Significant improvement in survival was noted in this treatment group ($p = 0.0007$), with an MS of 85.5 days. Three of six rats that received treatment at 0.8 mg nLs-CPT-11 by CED survived until termination of the study. The three remaining rats in this group were euthanized 54–62 days after tumor cell implantation due to neurological symptoms indicating tumor progression. Small tumors in the striatum were still evident in two of the surviving rats (Fig. 6D). Nevertheless, a significant survival benefit for nLs-CPT-11 over the control group was found (MS = 81 days; $p = 0.0016$). All rats in the group that received the combination treatment of Doxil and nLs-CPT-11 survived until the end of the study (MS > 100 days; $p < 0.0001$).

Next, we studied survival in rodents with U251MG brain tumor xenografts treated 14 days after tumor cell implantation. Rats in the control group that received drug-free liposomes were euthanized 38–46 days after tumor cell implantation due to neurological symptoms indicative of tumor progression (Fig. 4). The MS for the control group was 41 days. All animals receiving combination treatment of 0.8 mg nLs-CPT-11 and 2 mg Doxil survived 63–78 days, with an MS of 68 days ($p < 0.0001$).

A separate group of U87MG xenografts treated on day 10 was also evaluated. Rats in the control group that received drug-free liposomes were euthanized 18–21 days after implantation due to neurological symptoms indicative of tumor progression (MS = 19 days; Fig. 4). Five of six animals that received 2 mg Doxil were euthanized due to tumor-related symptoms 17–30 days after implantation (MS = 24 days). No significant survival benefit was observed for this group ($p = 0.215$). All animals that received 0.8 mg nLs-CPT-11 were euthanized due to neurological symptoms indicative of tumor

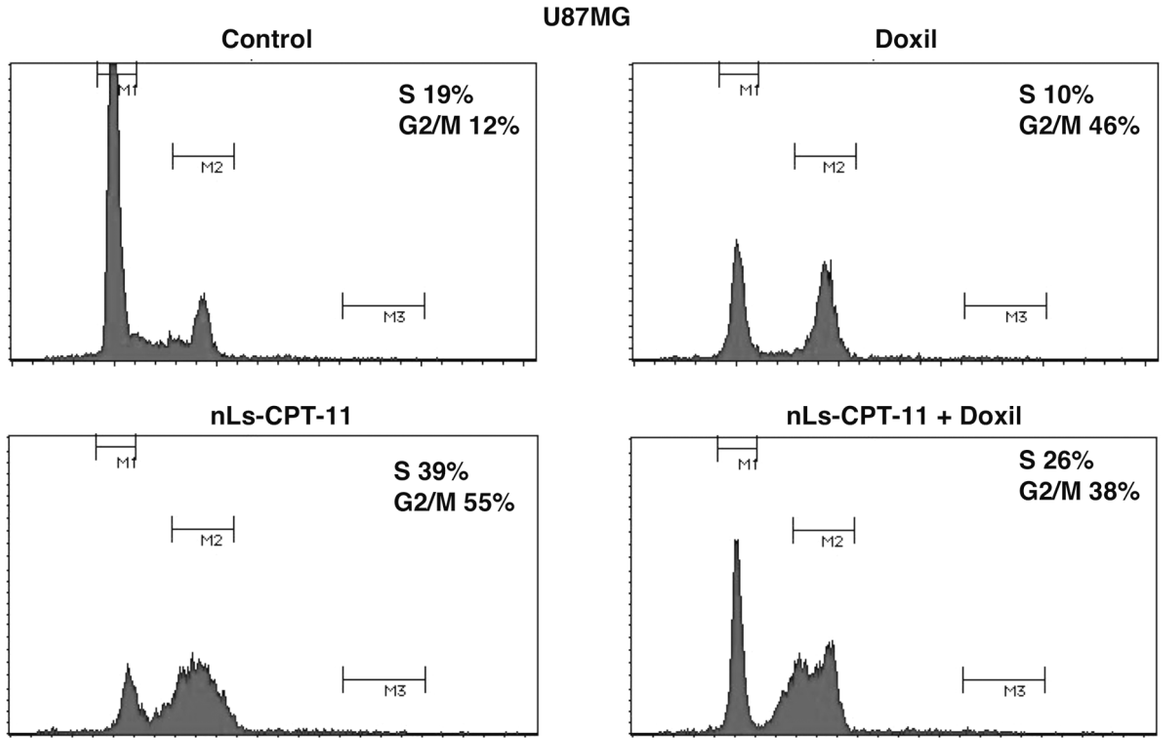

Fig. 2. Cell cycle profiles of U87MG cells examined by flow cytometry. U87MG cells were exposed to drug-free liposomes (control), Doxil (0.2 μg/ml), CPT-11 nanoliposomes (nLs-CPT-11) (5 μg/ml), or a combination of Doxil (0.2 μg/ml) and nLs-CPT-11 (5 μg/ml) for 24 h. Cells were harvested and analyzed by fluorescence-activated cell sorting as described in Materials and Methods.

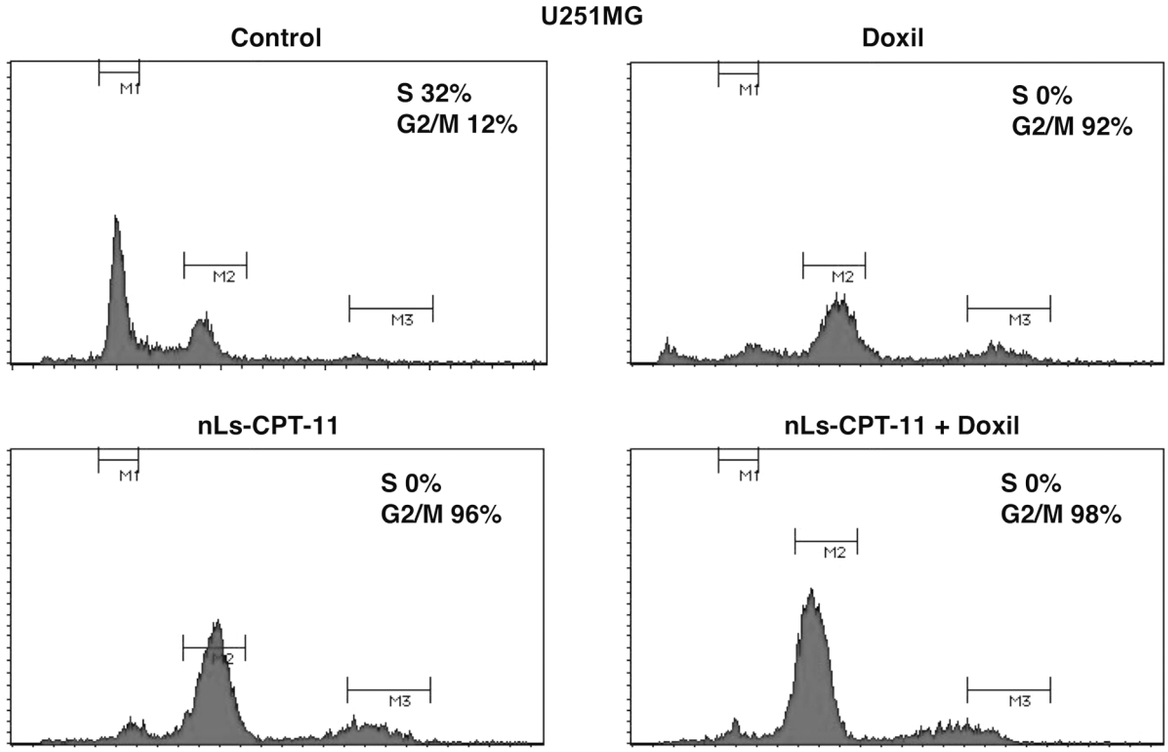

Fig. 3 Cell cycle profiles of U251MG cells examined by flow cytometry. U251MG cells were exposed to drug-free liposomes (control), Doxil (0.2 μg/ml), CPT-11 nanoliposomes (nLs-CPT-11; 5 μg/ml), or a combination of Doxil (0.2 μg/ml) and nLs-CPT-11 (5 μg/ml) for 24 h. Cells were harvested and analyzed by fluorescence-activated cell sorting as described in Materials and Methods.

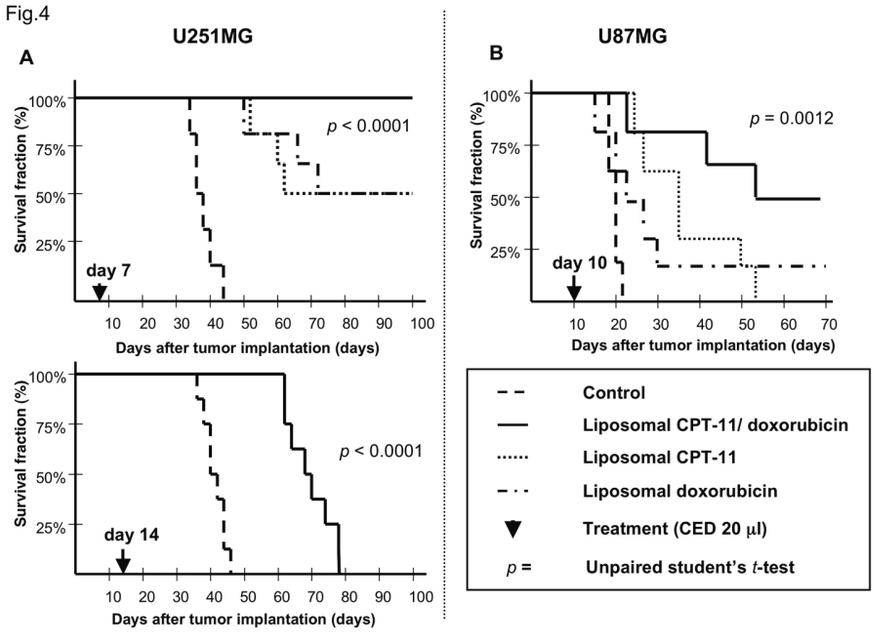

Fig. 4. Animals implanted with U251MG tumor cells. (A) Animals received liposome CED on day 7 and day 14 after tumor cell implantation. CED treatment on day 7 with nanoliposomal CPT-11 (nLs-CPT-11) and Doxil combination was able to eradicate all U251MG tumors in rodent striatum (see Fig. 5 caption). Each agent alone yielded only partial survival when delivered by CED on day 7. No animal in the day 14 combination therapy CED group survived longer than 78 days after tumor cell implantation. (B) Animals implanted with U87MG tumor cells received liposome CED on day 10 after tumor cell implantation. Three of six animals in the combination therapy group survived until termination of the study at day 70 after tumor cell implantation. Only one animal in the Doxil group survived until day 70. No animals in the nLs-CPT-11 group survived to the projected end of this survival study.

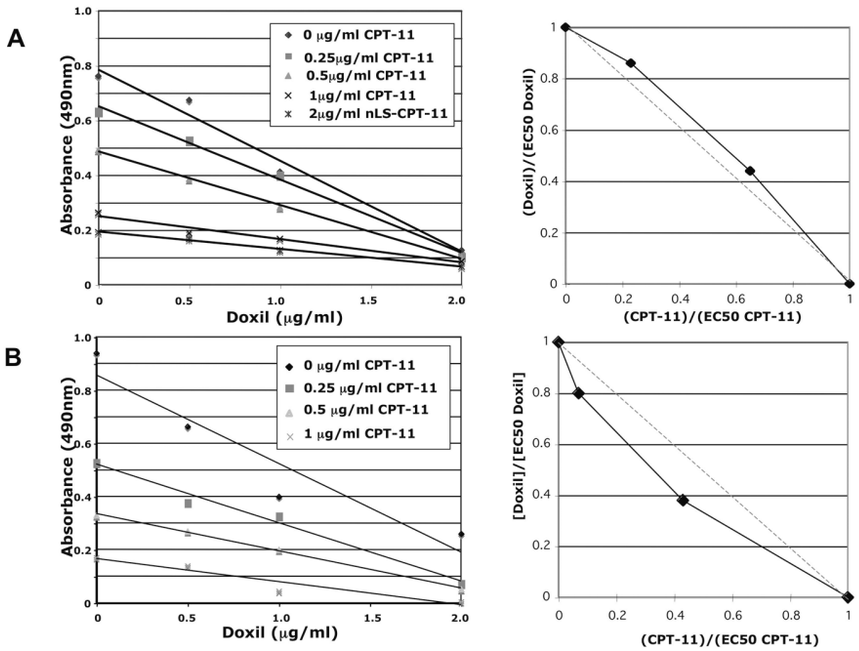

Fig. 5. Synergistic induction of cell death by Doxil and nanoliposomal CPT-11 (nLs-CPT-11) in U251MG glioma cells. (A) U87MG cells were treated for 24 h with increasing nLs-CPT-11 (0–2 µg/ml) concentrations and 24 h with increasing Doxil (0–2 µg/ml) concentrations. No synergy between the two agents was found by analysis of an isobologram (points above dotted line). (B) U251MG cells were treated identically to the U87MG cells with increasing Doxil and nLs-CPT-11 concentrations for 24 h. Synergy was determined between the two agents in the U251MG cell line as seen in the isobologram analysis (points below dotted line).

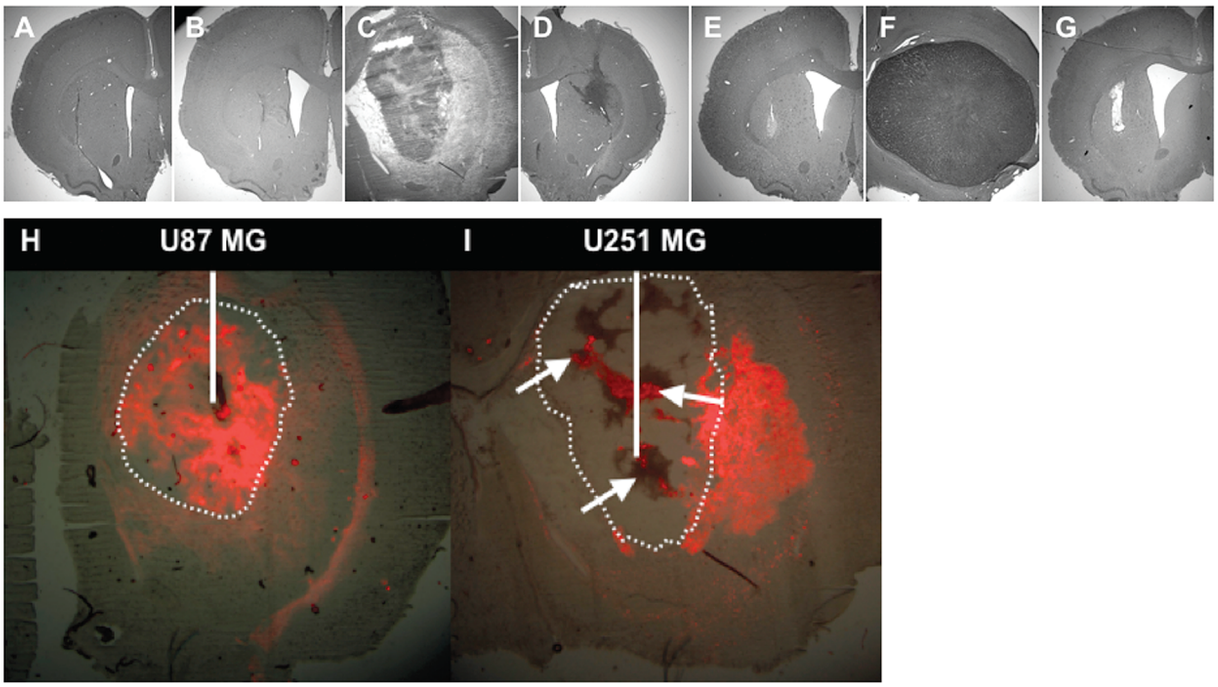

Fig. 6. Representative histology of animals used in this study. (A and B) Brain sections of animals used for toxicity study, euthanized 60 days after receiving the combination of Doxil (2.0 μg, 0.1 mg/ml) and nanoliposomal CPT-11 (nLs-CPT-11; 0.8 mg, 40 mg/ml). (C) Representative section of animals bearing U251MG xenografts. (D) Section from nLs-CPT-11 survivor of day 7 convection-enhanced delivery (CED) still bearing small U251MG tumor. (E) Survivor of day 7 CED combination therapy in U251MG at day 100. (F) Animal bearing U87MG xenografts. (G) Survivor of day 10 CED combination therapy in U87MG at day 70. (H and I) Representative sections showing $DiIC_{18}(3)$ fluorescent liposome distribution in U87MG (H) and U251MG (I) intracranial xenografts after 20 μl CED. White line represents infusion catheter placement; dotted line delineates tumor margin on histology sections; white arrows show necrotic areas in U251MG brain tumor xenografts.

progression 24–53 days after tumor cell implantation (MS = 30 days). CED treatment with nLs-CPT-11 alone resulted in a significant survival benefit ($p = 0.0048$). Three of six animals receiving combination therapy of 0.8 mg nLs-CPT-11 and 2 mg Doxil were euthanized 23–54 days after tumor cell implantation. Three animals survived until termination of the study 70 days after tumor cell implantation. A three-fold increase in mean survival was observed for the combination therapy group (MS = 62 days), compared to the control ($p = 0.0012$).

Distribution of Liposomes in U87MG and U251MG Brain Tumor Xenografts

After CED of 20 μl, liposomal $DiIC_{18}(3)$ distributed extensively throughout the U87MG brain tumor xenografts (Fig. 6H). However, the same amount of $DiIC_{18}(3)$ liposomes distributed mainly outside U251MG brain tumor xenografts and within necrotic areas (white arrows; Fig. 6I). The observed tumor-specific distribution highlights one contribution to variability in therapeutic efficacy between tumor models.

Discussion

Further improvement of current CED-based drug delivery protocols is critical for future clinical application. Clinical trials in which CED is employed for drug delivery to the brain have indicated considerable potential for this approach in neurooncology and in neurodegenerative diseases.[10,29] In this study, we have elucidated three important factors that affect overall survival: drug efficacy, drug tissue half-life, and drug distribution.

Liposomal encapsulation of chemotherapeutic drugs improves their pharmacokinetic properties.[14,20,21,30] An ideal combination of two liposomal chemotherapeutics would have similar half-lives in the CNS and rates of drug release from the carrier in order to exert maximum combined toxicity on tumor cells over extended periods of time. In our study, although the dose of Doxil used was 400-fold lower than that of nLs-CPT-11, their tissue half-lives were similar. Liposomal encapsulation not only enhances drug half-life but also improves distribution of compounds with high tissue affinity (e.g., Doxil),[9] as well as therapeutic index of the active agent (e.g., CPT-11).[8]

With respect to drug efficacy, we compared two brain tumor cell lines in our in vitro studies that are known to have different chemosensitivity in vitro.[31] The same dose of the drug combination that produced an intermediate response in U87MG caused almost complete G2 arrest in U251MG. Our drug combination showed synergy in the more chemosensitive cell line, U251MG, whereas no synergy was found in U87MG. Various mechanisms are known by which tumor cells escape G2 cell cycle arrest,[32,33] but different gene expression profiles, depending on whether cells are grown in vitro or in vivo, may be the key to the differences seen in this study.[34] Gene expression profiles in U87MG and U251MG, as determined by Camphausen et al.,[34] differ significantly in vitro but are similar when grown intracranially. We believe that contrast between the similar efficacy seen in the survival studies and the differences seen in our in vitro studies may be attributed to these effects. Moreover, the heterogeneity of malignant brain tumors warrants individual approaches to define the appropriate cancer treatment in each case.

We have shown previously that CED of liposomes easily covers an entire seven-day-old U251MG brain tumor xenograft (tumor diameter $\leqslant$0.5 mm).[35] The synergistic action of our liposomal therapeutic combination leads to complete eradication of U251MG xenografts, whereas Doxil or nLs-CPT-11 alone was only moderately efficacious. Interestingly, two of the three survivors in the nLs-CPT-11 group had relatively small tumor cell formations in the striatum at the termination of the study (day 100). Consistent with previous findings with nLs-CPT-11, we attribute this strong tumor growth inhibition in vivo to its central effect on the S-phase of the cell cycle.[8] In contrast, a survival study with 14-day-old U251MG brain tumor xenografts (vs. the seven-day xenografts; tumor diameter up to 1 mm) showed significant prolongation of survival. However, none of the animals survived past day 78 with the combination treatment. In order to explain this discrepancy, we conducted a series of liposome distribution studies in U251MG brain tumor xenografts. Large necrotic areas in U251MG brain tumor xenografts that increase with growth of the tumor appeared to alter liposome distribution within the tumor. As shown in Fig. 6, a large fraction of infused liposomes accumulated outside of the tumor or within necrotic areas. We conclude that the slow clearance of liposomal therapeutics inhibits tumor growth at its margins, but after eventual clearance of the therapeutic agents, tumor in areas not subject to liposome accumulation can lead to continued tumor growth. In the U87MG survival study, a significant extension of animal survival was also achieved, but only 50% of animals survived until termination of the study. As in the U251MG experiments, we also studied liposome distribution in U87MG brain tumor xenografts. Due to its rather homogeneous growth pattern, good distribution of liposomes was observed in U87MG xenografts (tumor diameter ~ 1.5 mm on day 10).[35] However, despite the better distribution of liposomes in U87MG tumors, the fast growth of U87MG, the slow release of therapeutics from liposomes, and the lower sensitivity to Doxil/nLs-CPT-11 combination in vitro, compared with U251MG, all contribute to reduced efficacy in U87MG versus U251MG tumors.

Several important conclusions can be drawn from this study. For patients with brain tumors, systemic delivery of therapeutics is usually associated with systemic side effects while achieving only marginal therapeutic concentrations in the CNS. This limits the effectiveness of systemic treatment. Thus, clinical trials to evaluate the combination of Topo I and II inhibitors via intravenous administration in patients with solid neoplasms demonstrated substantial toxicity.[23,24] The defined MTD was frequently lower than the typical dose level for the respective individual agent. CED of nonencapsulated chemotherapeutic agents has produced better outcomes but was also highly toxic upon extensive distribution of free drug within the CNS.[36] CED of a mixture of Doxil and nLs-CPT-11 has shown excellent therapeutic potential without signs of toxicity to the CNS at the doses of each liposomal drug employed. Both therapeutics were used at doses previously shown to be individually nontoxic but to be substantially therapeutic in brain tumors when delivered by CED.[8,9] The present drug combination was therefore capable of increasing therapeutic efficacy by synergistic action in U251MG without increase in CNS toxicity. Although synergy was not formally demonstrated via isobologram analysis in U87MG in vitro, the combination therapy in vivo nevertheless resulted in improved survival over each agent alone.

Another important aspect of this study is the prolonged release of the two drugs from liposomes.[8] This slow-release phenomenon might benefit patients with brain tumors, since human tumors grow far more slowly than do animal tumor xenografts. As shown by our animal experiments, eradication of tumor is a realistic possibility only when complete coverage with a liposomal drug is achieved. This is why we have developed a real-time imaging method to visualize direct liposome delivery into the CNS.[17,19] This real-time imaging technique, in combination with several infusion catheters, may permit complete liposomal coverage of tumors in human brain, because the drug may then be infused until optimal distribution is achieved while avoiding untoward leakage of the drug into healthy surrounding tissue. Currently, we are undertaking experiments in canine de novo brain tumors in order to validate the present rodent experiments in a larger mammalian brain and to strengthen the hypothesis that distribution of liposomes in tumors is greatly affected by tumor histology. Although all studies were conducted on a relatively small number of animals per group, our findings were consistent with previous rodent and primate studies. In the human setting, malignant tumors are usually more than 1 cm in diameter at time of diagnosis, and are located in various parts of the brain. Our previous studies on naive primate brains have clearly shown that our CED delivery technique, when combined with our step cannula design, allows liposome delivery into every CNS structure at any given depth.[17,19] Application of this delivery technique will probably require multiple cannulas in order to cover the entire tumor mass. We

are aware that more work needs to be done in the field of distribution characterization as a function of tumor histology, but a more complete conceptual understanding of liposome therapeutics and distribution has now been established.

Acknowledgments

This work was supported by grants from the National Cancer Institute Specialized Program of Research Excellence grant (K.S.B. and J.W.P.) and Accelerate Brain Cancer Cure (K.S.B.).

References

1. Groothuis DR. The blood-brain and blood-tumor barriers: a review of strategies for increasing drug delivery. *Neuro-Oncology*. 2000;2:45–59.
2. Huynh GH, Deen DF, Szoka FC Jr. Barriers to carrier mediated drug and gene delivery to brain tumors. *J Control Release*. 2006;110:236–259.
3. Walter KA, Tamargo RJ, Olivi A, Burger PC, Brem H. Intratumoral chemotherapy. *Neurosurgery*. 1995;37:1128–1145.
4. Giese A, Kucinski T, Knopp U, et al. Pattern of recurrence following local chemotherapy with biodegradable carmustine (BCNU) implants in patients with glioblastoma. *J Neurooncol*. 2004;66:351–360.
5. Bobo RH, Laske DW, Akbasak A, Morrison PF, Dedrick RL, Oldfield EH. Convection-enhanced delivery of macromolecules in the brain. *Proc Natl Acad Sci U S A*. 1994;91:2076–2080.
6. Saito R, Bringas JR, Panner A, et al. Convection-enhanced delivery of tumor necrosis factor-related apoptosis-inducing ligand with systemic administration of temozolomide prolongs survival in an intracranial glioblastoma xenograft model. *Cancer Res*. 2004;64:6858–6862.
7. Kioi M, Husain SR, Croteau D, Kunwar S, Puri RK. Convection-enhanced delivery of interleukin-13 receptor-directed cytotoxin for malignant glioma therapy. *Technol Cancer Res Treat*. 2006;5:239–250.
8. Noble CO, Krauze MT, Drummond DC, et al. Novel nanoliposomal CPT-11 infused by convection-enhanced delivery in intracranial tumors: pharmacology and efficacy. *Cancer Res*. 2006;66:2801–2806.
9. Yamashita Y, Saito R, Krauze MT, Noble CO, Kawaguchi T, Bankiewicz KS. Convection-enhanced delivery of liposomal doxorubicin in intracranial brain tumor xenografts. *Targeted Oncol*. 2006;1:79–85.
10. Kunwar S. Convection enhanced delivery of IL13-PE38QQR for treatment of recurrent malignant glioma: presentation of interim findings from ongoing phase 1 studies. *Acta Neurochir* 2003;88(suppl):105–111.
11. Carpentier A, Laigle-Donadey F, Zohar S, et al. Phase 1 trial of a CpG oligodeoxynucleotide for patients with recurrent glioblastoma. *Neuro-Oncology*. 2006;8:60–66.
12. Vogelbaum MA. Convection enhanced delivery for the treatment of malignant gliomas: symposium review. *J Neurooncol*. 2005;73:57–69.
13. Mardor Y, Roth Y, Lidar Z, et al. Monitoring response to convection-enhanced taxol delivery in brain tumor patients using diffusion-weighted magnetic resonance imaging. *Cancer Res*. 2001;61:4971–4973.
14. Drummond DC, Meyer O, Hong K, Kirpotin DB, Papahadjopoulos D. Optimizing liposomes for delivery of chemotherapeutic agents to solid tumors. *Pharmacol Rev*. 1999;51:691–743.
15. Allen TM, Cullis PR. Drug delivery systems: entering the mainstream. *Science*. 2004;303:1818–1822.
16. Saito R, Bringas JR, McKnight TR, et al. Distribution of liposomes into brain and rat brain tumor models by convection-enhanced delivery monitored with magnetic resonance imaging. *Cancer Res*. 2004;64:2572–2579.
17. Krauze MT, McKnight TR, Yamashita Y, et al. Real-time visualization and characterization of liposomal delivery into the monkey brain by magnetic resonance imaging. *Brain Res Brain Res Protoc*. 2005;16:20–26.
18. Krauze MT, Saito R, Noble C, et al. Reflux-free cannula for convection-enhanced high-speed delivery of therapeutic agents. *J Neurosurg*. 2005;103:923–929.
19. Saito R, Krauze MT, Bringas JR, et al. Gadolinium-loaded liposomes allow for real-time magnetic resonance imaging of convection-enhanced delivery in the primate brain. *Exp Neurol*. 2005;196:381–389.
20. Drummond DC, Marx C, Guo Z, et al. Enhanced pharmacodynamic and antitumor properties of a histone deacetylase inhibitor encapsulated in liposomes or ErbB2-targeted immunoliposomes. *Clin Cancer Res*. 2005;11:3392–3401.
21. Drummond DC, Noble CO, Guo Z, Hong K, Park JW, Kirpotin DB. Development of a highly active nanoliposomal irinotecan using a novel intraliposomal stabilization strategy. *Cancer Res*. 2006;66:3271–3277.
22. Saito R, Krauze MT, Noble CO, et al. Convection-enhanced delivery of Ls-TPT enables an effective, continuous, low-dose chemotherapy against malignant glioma xenograft model. *Neuro-Oncology*. 2006;8:205–214.
23. Ando M, Eguchi K, Shinkai T, et al. Phase I study of sequentially administered topoisomerase I inhibitor (irinotecan) and topoisomerase II inhibitor (etoposide) for metastatic non-small-cell lung cancer. *Br J Cancer*. 1997;76:1494–1499.
24. Herben VM, ten Bokkel Huinink WW, Dubbelman AC, et al. Phase I and pharmacological study of sequential intravenous topotecan and oral etoposide. *Br J Cancer*. 1997;76:1500–1508.
25. Hammond LA, Eckardt JR, Ganapathi R, et al. A phase I and translational study of sequential administration of the topoisomerase I and II inhibitors topotecan and etoposide. *Clin Cancer Res*. 1998;4:1459–1467.

26. Bartlett GR. Colorimetric assay methods for free and phosphorylated glyceric acids. *J Biol Chem*. 1959;234:469–471.
27. Bankiewicz KS, Eberling JL, Kohutnicka M, et al. Convection-enhanced delivery of AAV vector in parkinsonian monkeys; in vivo detection of gene expression and restoration of dopaminergic function using prodrug approach. *Exp Neurol*. 2000;164:2–14.
28. Berenbaum MC. Criteria for analyzing interactions between biologically active agents. *Adv Cancer Res*. 1981;35:269–335.
29. Lang AE, Gill S, Patel NK, et al. Randomized controlled trial of intraputamenal glial cell line-derived neurotrophic factor infusion in Parkinson disease. *Ann Neurol*. 2006;59:459–466.
30. Allen TM, Hansen CB, Lopes de Menezes DE. Pharmacokinetics of long-circulating liposomes. *Adv Drug Del Rev*. 1995;16:267–284.
31. Wolff JE, Trilling T, Molenkamp G, Egeler RM, Jurgens H. Chemosensitivity of glioma cells in vitro: a meta analysis. *J Cancer Res Clin Oncol*. 1999;125:481–486.
32. Walker DH, Adami GR, Dold KM, Babiss LE. Misregulated expression of the cyclin dependent kinase 2 protein in human fibroblasts is accompanied by the inability to maintain a G2 arrest following DNA damage. *Cell Growth Differ*. 1995;6:1053–1061.
33. Karlseder J, Wissing D, Holzer G, et al. HSP70 overexpression mediates the escape of a doxorubicin-induced G2 cell cycle arrest. *Biochem Biophys Res Commun*. 1996;220:153–159.
34. Camphausen K, Purow B, Sproull M, et al. Influence of in vivo growth on human glioma cell line gene expression: convergent profiles under orthotopic conditions. *Proc Natl Acad Sci U S A*. 2005;102:8287–8292.
35. Yamashita Y, Krauze MT, Kawaguchi T, et al. Convection-enhanced delivery of a topoisomerase I inhibitor (nanoliposomal topotecan) and a topoisomerase II inhibitor (pegylated liposomal doxorubicin) in intracranial brain tumor xenografts. *Neuro-Oncology*. 2007;9:20–28.
36. Kaiser MG, Parsa AT, Fine RL, Hall JS, Chakrabarti I, Bruce JN. Tissue distribution and antitumor activity of topotecan delivered by intracerebral clysis in a rat glioma model. *Neurosurgery*. 2000;47:1391–1399.